Giant tunnelling magnetoresistance at room temperature with MgO (100) tunnel barriers

STUART S. P. PARKIN[1]*, CHRISTIAN KAISER[1], ALEX PANCHULA[1], PHILIP M. RICE[1], BRIAN HUGHES[2], MAHESH SAMANT[1] AND SEE-HUN YANG[1]

[1]IBM Research Division, [2]Infineon Technologies, IBM Almaden Research Center, IBM-Infineon MRAM Development Alliance, 650 Harry Road, San Jose, California 95120, USA
*e-mail: parkin@almaden.ibm.com

Published online: 31 October 2004; doi:10.1038/nmat1256

Magnetically engineered magnetic tunnel junctions (MTJs) show promise as non-volatile storage cells in high-performance solid-state magnetic random access memories (MRAM)[1]. The performance of these devices is currently limited by the modest (<~70%) room-temperature tunnelling magnetoresistance (TMR) of technologically relevant MTJs. Much higher TMR values have been theoretically predicted for perfectly ordered (100) oriented single-crystalline Fe/MgO/Fe MTJs. Here we show that sputter-deposited polycrystalline MTJs grown on an amorphous underlayer, but with highly oriented (100) MgO tunnel barriers and CoFe electrodes, exhibit TMR values of up to ~220% at room temperature and ~300% at low temperatures. Consistent with these high TMR values, superconducting tunnelling spectroscopy experiments indicate that the tunnelling current has a very high spin polarization of ~85%, which rivals that previously observed only using half-metallic ferromagnets[2]. Such high values of spin polarization and TMR in readily manufactureable and highly thermally stable devices (up to 400 °C) will accelerate the development of new families of spintronic devices.

The basic element of an MTJ is a sandwich of two ferromagnetic (F) electrodes separated by a thin insulating tunnel barrier[1]. The tunnel current through the barrier depends on the relative orientation of the magnetic moments of the electrodes, giving rise to a TMR, typically defined as $(R_{AP}–R_P)/R_P$, where R_{AP} and R_P are the resistances for anti-parallel (AP) and parallel (P) alignment of the magnetic moments, respectively[3–5]. The magnitude of the TMR is directly related to the spin polarization of the tunnelling electrons[6], which itself is determined by the spin dependence of the density of states near the Fermi energy of each of the ferromagnetic electrodes, and the tunnelling matrix elements for these electrons[7]. Thus, the higher the tunnelling spin polarization (TSP), the higher the TMR, so that there has been considerable interest in nominally half-metallic ferromagnetic electrodes, such as the manganite perovskites[8–10] and CrO_2 (ref. 2). However, although TMR values of ~1,000%[8,11] and TSP values of ~70%[12] have been measured at low temperatures in tunnel junctions with electrodes formed from the perovskite manganites, very small effects are found at room temperature, only partly accounted for by the low Curie temperature of these ferromagnets.

By contrast, conventional ferromagnetic metals formed from Fe, Co and Ni have much higher Curie temperatures—well above room temperature. Just as important, by using the phenomenon of oscillatory interlayer coupling in transition metal multilayers[13], useful magnetic structures for technological applications can be readily magnetically engineered from thin layers of these ferromagnets[1]. However, after several decades of work, the highest TSP found in technologically useful tunnel junctions incorporating these metals is ~55% for alumina tunnel barriers[1,6], with corresponding TMR values in MTJs of up to ~70% at room temperature[14].

Alumina tunnel barriers are amorphous. It has been predicted that crystalline tunnel barriers may give rise to much higher TSP and TMR values because of a highly spin-dependent evanescent decay of certain wave-functions, with particular transverse momentum values, across the tunnel barrier[15]. In particular, calculations for perfectly ordered (100) oriented Fe/MgO/Fe MTJs, suggest TMR values of hundreds or even thousands of percent, for sufficiently thick MgO tunnel barriers[16,17]. If these giant values could be realized, the impact on various information storage technologies would be immense, for example, MRAM with read performance an order of magnitude greater than current prototypes. This has motivated intense research activities over the past several years on epitaxial MTJs grown on single-crystalline substrates using molecular beam epitaxy deposition techniques. None of them[18–20], however, has demonstrated TMR values much higher than those that can achieved with alumina tunnel barriers (88% versus 70%). Here we show MTJs with giant TMR values several times higher than previously observed, fabricated using simple sputter-deposition techniques at ambient temperature on amorphous substrate layers. Moreover, these devices show remarkable thermal stability making them suitable for integration with CMOS circuits for MRAM applications.

Typical resistance versus field curves are shown in Fig. 1 for three similar MTJs with lower ferromagnetic electrodes formed from Fe and $Co_{70}Fe_{30}$, patterned by *in situ* shadow-masks to give junction areas of 80 × 80 μm^2. Very large TMR values ranging from ~120% to more than 165% at room temperature are found. The MTJs were prepared, nominally at ambient temperature, by sputter deposition using a combination of ion-beam and magnetron sputtering. The lower ferromagnetic electrode is formed by first depositing an

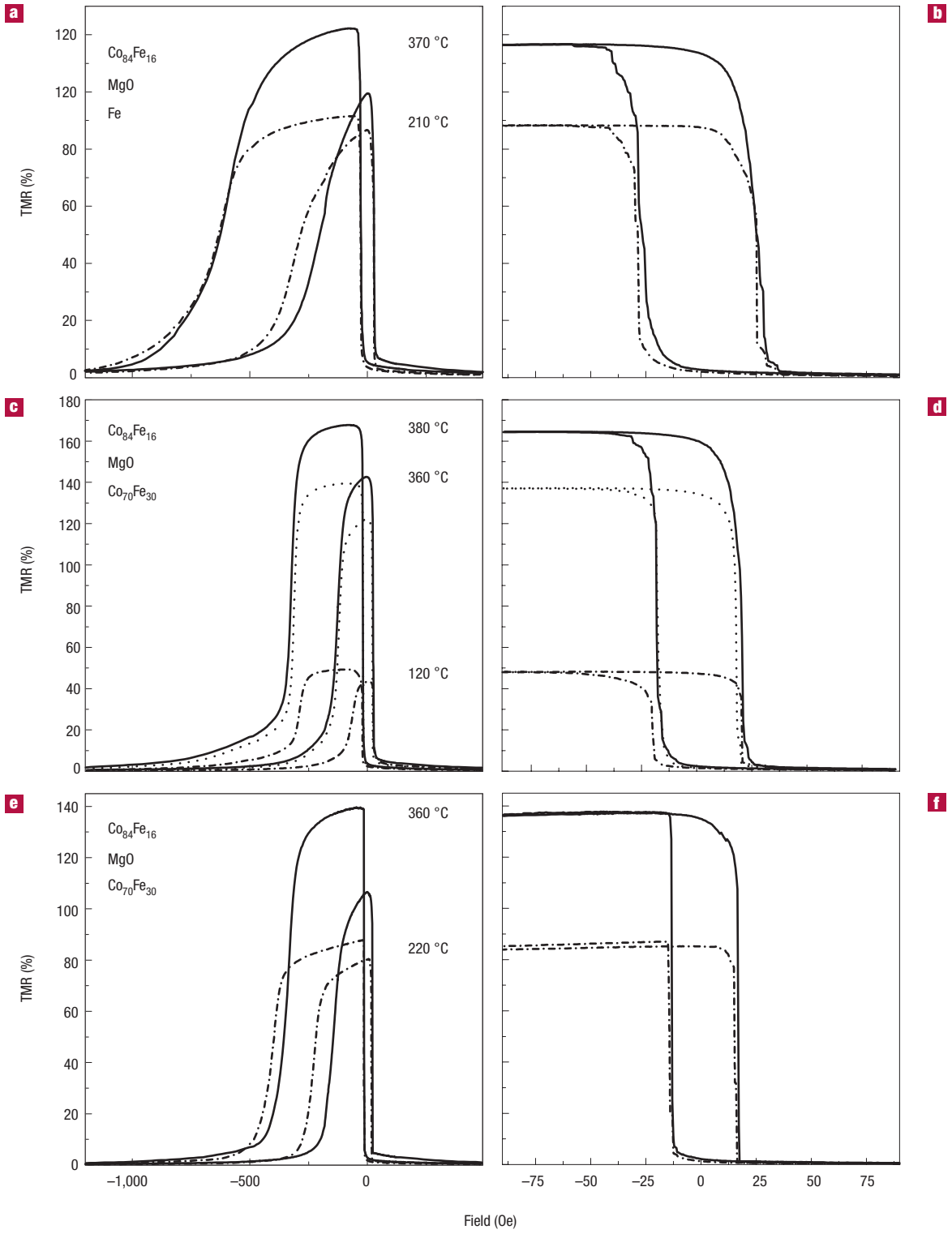

Figure 1 Giant room-temperature TMR. Plots of TMR versus field for MTJs with structures as follows (all thicknesses in ångströms): **a** and **b**, 100 TaN / 250 IrMn/ 8 $Co_{84}Fe_{16}$/ 18 Fe/ 27 MgO/ 100$Co_{84}Fe_{16}$/ 100 TaN. **c** and **d**, 100 TaN / 250 IrMn/ 8 $Co_{84}Fe_{16}$/ 30 $Co_{70}Fe_{30}$/ 29 MgO/ 150 $Co_{84}Fe_{16}$/ 100 Mg. **e** and **f**, 100 TaN / 250 IrMn/ 8 $Co_{84}Fe_{16}$/ 30 $Co_{70}Fe_{30}$/ 31 MgO/ 150 $Co_{84}Fe_{16}$/ 125 TaN. The corresponding final anneal temperature T_A, after which the data is measured at room temperature, is shown in the figure. The field range in **a**, **c** and **e** is sufficiently broad that both the switching of the exchanged biased lower ferromagnetic electrode and the upper ferromagnetic electrodes are seen, whereas data in **b**, **d** and **f** correspond to a minor hysteresis loop where the field range is limited so that only the upper electrode switches. The exchange bias field is larger in **a** than in **c** and **e** because of the thinner ferromagnetic electrode in **a**. The resistance and *RA* values of the MTJs in high field and after annealing at the highest temperature shown are: **a** and **b,** 720 Ω and 4,600 kΩ μm^2, **c** and **d,** 30 Ω and 175 kΩ μm^2, **e** and **f** ,10,250 Ω and 65,600 kΩ μm^2, respectively. Note that the junction in **e** and **f** has a resistance ~400 times higher than that in **c** and **d** but the TMR data are very similar after annealing to the same temperature of 360 °C.

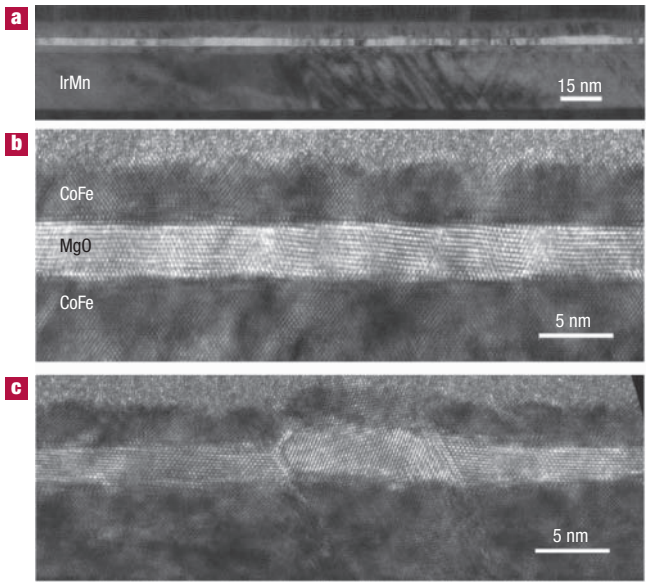

Figure 2 Highly oriented (100) MgO tunnel barrier. Transmission electron micrographs of magnetic tunnel junctions. **a**, Low-magnification image showing the growth of ultra-smooth underlayers formed from TaN, Ta, IrMn and CoFe, each readily distinguishable, which form a template for the growth of the (100) oriented MgO tunnel barrier (lightest layer), **b** and **c**, High-resolution images along the [110] zone axes showing atomically resolved lattice planes with (100) planes perpendicular to the growth direction. The (100) planes in the grain in the centre of **c** are rotated by ~–15°. Diffractograms show that the MgO lattice is compressed in-plane by ~2% with respect to bulk MgO ($d_{022} \approx 1.46 \pm 0.02$ Å versus 1.49 Å), presumably due to strain from the lower CoFe electrode ($d_{002} \approx 1.40 \pm 0.02$ Å) and that the [011] MgO axis is aligned along CoFe [001], as previously observed for epitaxial growth of MgO on Fe(001)[30]. The MgO lattice is correspondingly expanded out of plane by ~2.5% (MgO: $d_{200} \approx 2.16 \pm 0.02$ Å).

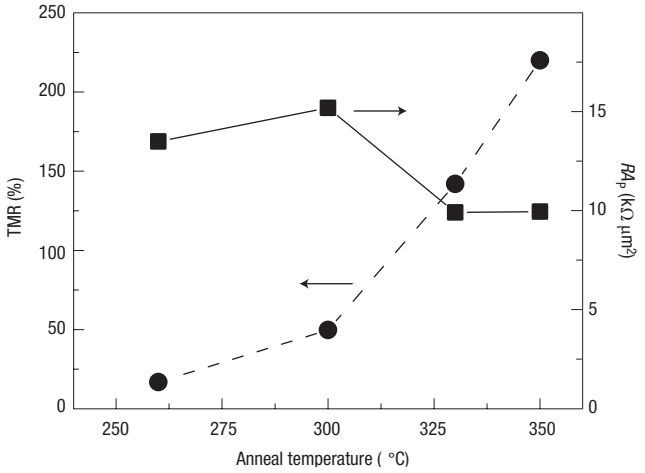

Figure 3 Anneal dependence of TMR and *RA* measured using the current-in-plane tunnelling measurement technique on an unpatterned MTJ film. TMR and *RA* in the parallel state, RA_P, measured at room temperature versus anneal temperature. The MgO tunnel barrier is ~20 Å thick. The structure is similar to that of Fig. 1e except that the IrMn layer is ~150 Å thick, the lower electrode comprises 35 Å $Co_{70}Fe_{30}$, and the upper electrode comprises 75 Å of $(Co_{70}Fe_{30})_{80}B_{20}$. In addition a 75 Å Ru cap layer is used for improved electrical contacts. The parallel state *RA* product is ~10^4 Ω μm², which is about 20 times smaller than the sample of Fig. 1c and d due to the smaller MgO thickness. After annealing at 350 °C the TMR attains a value of 220 ± 10%.

underlayer of 100 Å TaN on an amorphous layer of SiO_2 formed on a Si(100) substrate. An antiferromagnetic layer of 250 Å $Ir_{22}Mn_{78}$, which is used to exchange bias the lower ferromagnetic layer[1], is then deposited by ion-beam sputtering, followed by the ferromagnetic layer, which is formed from a bilayer of 8Å $Co_{84}Fe_{16}$ and either 18 Å Fe (Fig. 1a and b) or 30Å $Co_{70}Fe_{30}$ (Fig. 1c–f). The MgO tunnel barrier is formed by reactive magnetron sputtering in an argon–oxygen mixture (3 mtorr). Growth conditions were optimized to give nearly stochiometric MgO. The barrier was also prepared by a variety of other techniques including ion-beam sputtering, thermal evaporation and electron beam evaporation. The usage of shadow-masked junctions allows us to explore a wide variety of deposition conditions and techniques and to optimize each one. The upper ferromagnetic electrode is formed from a layer of $Co_{84}Fe_{16}$ with capping layers formed from TaN or Mg. The highest TMR values were found for MTJs with Co-rich Co–Fe electrodes. MTJs with Fe electrodes systematically gave lower TMR values.

Transmission electron micrographs show an excellent morphology of the MTJ structures with extremely smooth and flat layers as shown in the micrograph in Fig. 2a. Diffractograms (not shown) from selected areas of the digital micrograph reveal that the IrMn layer is f.c.c. with a (100) texture. High-resolution micrographs show a high degree of epitaxy of the MgO and upper and lower Co–Fe layers as shown in Fig. 2b. Both the Co–Fe layers are b.c.c. with a (100) texture and the MgO is cubic (NaCl structure) and also (100) textured. Although the structures are highly (100) textured they are polycrystalline with random in-plane orientations and are structurally imperfect. For example, a significant number of defects along the (111) planes in the IrMn layer, most likely stacking faults, can be seen in Fig. 2a and at higher magnification in Fig. 2c. The stacking faults propagate from the IrMn layer through the MgO tunnel barrier to the upper CoFe layer.

The TMR of the MTJs, as deposited, is modest but is dramatically increased by thermal annealing in vacuum at temperatures of up to ~400 °C. Typically, the TMR increases monotonically and almost linearly with increasing anneal temperature, whereas the resistance of the junction changes little up to a critical temperature, in the range ~350–425 °C. Above this temperature the junction fails with a loss of both resistance and TMR. The three junctions shown in Fig. 1 survived to anneal temperatures of ~370 °C, 380 °C and 360 °C, respectively, with respective TMR values of 123%, 168% and 140%.

The dependence of TMR on MgO barrier thickness was explored using both shadow-masked junctions, and, at room temperature, by the technique of current-in-plane tunnelling (CIPT)[22] on unpatterned films where the MgO thickness was linearly increased across the wafer. The CIPT technique, using an array of 12 microscopic probes, allows the study of junctions with much lower resistance–area (*RA*) products (thinner MgO barriers), and has been demonstrated to give highly reliable values of TMR, where the analysis[21] exactly takes into account the value of *RA* and the resistance per square $R_\square$ of the top and bottom electrodes. Both techniques give similar TMR values for MTJs with similar *RA* values (~160% for *RA*~10^5 Ω μm²). No significant variation of TMR with MgO barrier thickness was found, contrary to theoretical predictions of rapidly increasing TMR with MgO thickness for epitaxial Fe/MgO/Fe (ref. 16). TMR values as high as 220±10% were found by CIPT for MTJ stacks with $RA \approx 10^4$ Ω μm² after an anneal at 350 °C, as shown in Fig. 3.

The TMR was found to decrease with bias voltage, as is typically seen for MTJs, dropping to half at a voltage of ~0.3 to 0.6 volts, symmetrically for both positive and negative voltage. The effective

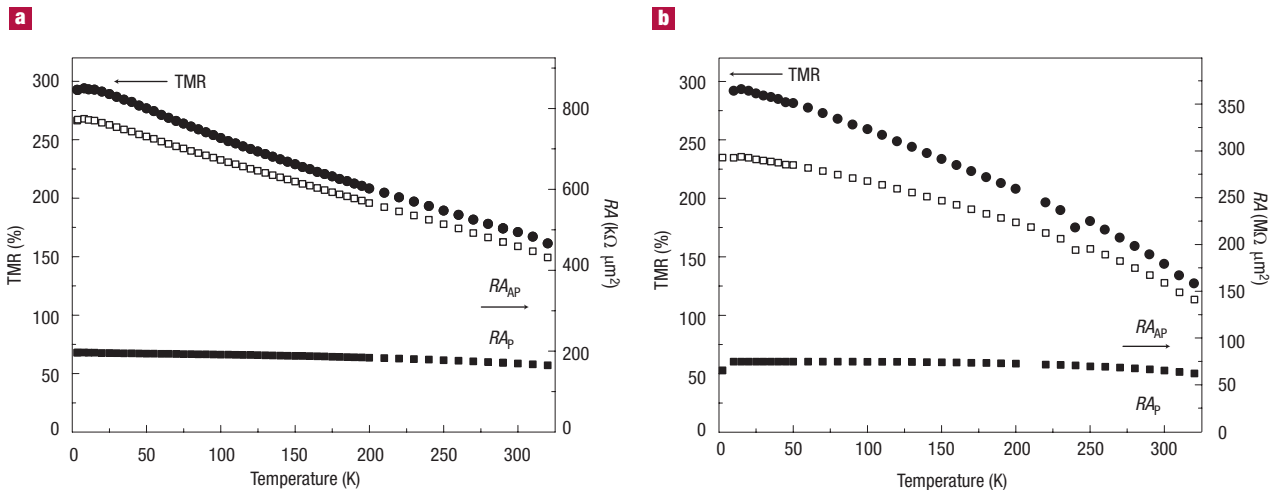

Figure 4 Temperature dependence of TMR (filled circles) and *RA* (squares) for the same magnetic tunnel junctions shown in Fig. 1. a, Sample from Fig. 1c and d (annealed at 380 °C). **b**, Sample from Fig. 1e and f (annealed at 360 °C) in magnetic fields of –100 and +1,000 Oe to set the state of the junction in the anti-parallel (AP) and parallel (P) states, respectively. The TMR values are extracted from measuring the resistance versus field loop at each temperature.

height of the MgO tunnel barrier, deduced from current versus voltage curves[22], was ~1.1 to 1.7 volts, in agreement with previous electrical studies on MgO barriers[23,24]. However, these values are much smaller than those we infer from valence band photoemission experiments on similar MTJ structures but deposited without the upper electrode. The latter clearly shows that the top of the MgO valence band is ~3.5 eV below the Co–Fe Fermi energy, consistent with the band structure of bulk MgO (ref. 26), assuming that the Fermi level is pinned mid-gap. The significant discrepancy between the transport and electronic structure studies suggests that the MgO barriers contain defect states.

It has long been realized that the resistance of tunnelling junctions[26] and the TMR of MTJs can be affected by current crowding effects if the resistance of the electrodes is comparable to the resistance of the tunnel junction itself. For MTJs this can lead to artificially high TMR values. Careful attention was paid to ensure that the extraordinarily high TMR values we find are not significantly affected by current crowding. First, the CIPT technique is immune to this effect. Second, the high TMR values were observed for a wide range of MgO thickness for otherwise the same electrode $R_{\square}$ values. In particular, as shown in Fig. 1c–f, two junctions with otherwise the same structure but with slightly different MgO barrier thicknesses give the same TMR values (~140%) after similar anneal treatments (at 360 °C). The ratio of the junction resistance to $R_{\square}$ is ~6 and ~2,000 for these two junctions, respectively. Current crowding effects can unambiguously be ruled out for the latter junction and are at most a 5% effect for the former[27]. Moreover, high TMR values of more than 130% have been confirmed in lithographically patterned junctions in MRAM test chips with RA ~10^4 Ω μm^2 and areas as small as 0.06 μm^2, where again there is no possible current crowding effect. These MTJs had ferromagnetic electrodes as thin as 15 Å thick: no significant dependence of TMR on electrode thickness was found.

Figure 4 shows the TMR and *RA* of the two junctions of Fig. 1c–f as a function of temperature. The TMR increases as the temperature is reduced attaining a value of ~300% at 4 K for each junction. The increase in TMR results from an increase of the resistance of the AP state of the junction R_{AP} whereas the P state resistance R_P hardly changes at all on cooling. With increasing temperature, increasing magnetic disorder will decrease R_{AP} but should increase R_P, whereas, by contrast, thermal excitations across the barrier will decrease both R_{AP} and R_P. Thus, the weak dependence of R_P is probably a coincidental cancellation of these two effects.

The magnitude of the spin polarization of the tunnelling current was measured at low temperature using the superconducting tunnelling spectroscopy (STS) technique[6]. To use this technique the upper ferromagnetic electrode was replaced by a thin layer of $Al_{96}Si_4$ which is superconducting at the measurement temperature of ~0.25 K. In the presence of a large magnetic field (2 T) the quasi-particle density of states in the superconductor is Zeeman-split providing for spin-polarized states into which the electrons tunnel. Thus the superconducting electrode serves as an analyser of the spin polarization of the tunnelling current. By fitting the conductance versus bias voltage curves the TSP can be inferred with high precision[1,6,7,12]. Results for Fe and $Co_{70}Fe_{30}$ electrodes are shown in Fig. 5. As deposited, these electrodes have TSP values of ~57% and 52%, but after annealing, these values increase dramatically, attaining values of ~74% and 85% at anneal temperatures of 380 and 410 °C, respectively. These values are almost twice as high as those found for the same ferromagnets with alumina tunnel barriers[1,6]. Moreover, these results demonstrate that a ferromagnetic metal does not have a unique, direction-independent, spin-polarization value, as has long been assumed. Similar conclusions have previously been inferred from changes in the sign of TMR for junctions containing $SrTiO_3$ barriers and Co and manganite ferromagnetic electrodes[28].

The Julliere model[3,6,7] is often used to relate tunnelling spin-polarization with TMR. In this model a TSP of 85% would give rise to a TMR of ~520% at low temperatures. Furthermore, if we assume a similar temperature dependence to that shown in Fig. 4, TMR values of more than 260% at room temperature are predicted from the TSP values. Such TMR values are very close to the highest TMR values we have measured in MTJs. In any case STS measurements will likely give rise to higher TSP values than those inferred from TMR, because the AP alignment of the ferromagnetic electrodes in the latter is unlikely to be perfect, whereas the large magnetic fields used in the TSP studies ensure almost complete alignment of the ferromagnetic electrode moment with the magnetic field.

In conclusion, we have demonstrated remarkably high tunnelling magnetoresistance values ranging from ~120% to 220% at room temperature in sputter-deposited (100) oriented CoFe/MgO/CoFe magnetic tunnelling junctions prepared on amorphous substrates.

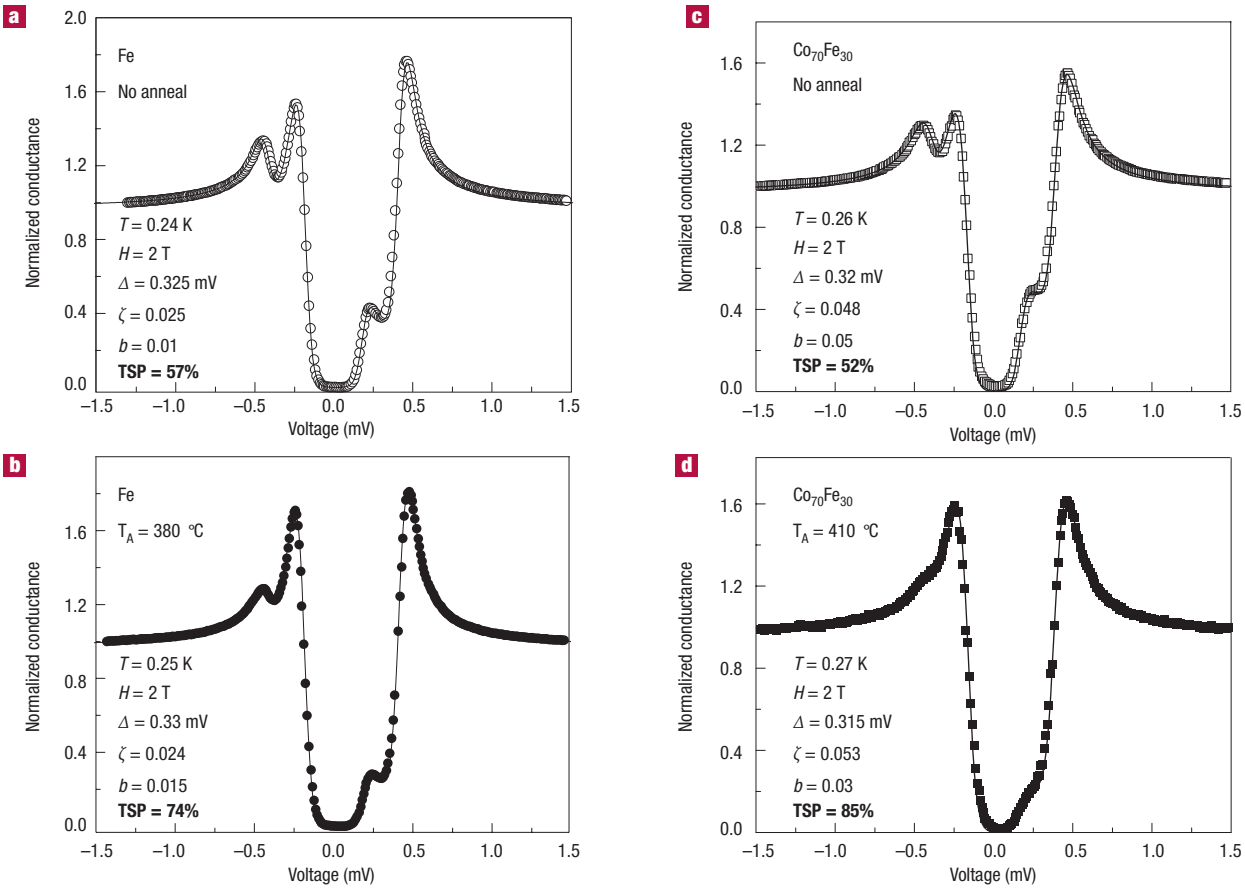

Figure 5 Measurement of tunnelling spin-polarization. Conductance versus bias voltage curves (symbols) and fits (solid lines) for STS junctions with superconducting counter electrodes of $Al_{96}Si_4$ and: **a** and **b**, Fe, and **c** and **d**, $Co_{70}Fe_{30}$ ferromagnetic electrodes. **a** and **c** correspond to the as-deposited junctions (no anneal), and **b** and **d** to junctions annealed at 380 °C and 410 °C, respectively. The resistance of the junctions in each case exceeds~10,000 Ω. The measurements were taken at ~0.25K in a field of 2T applied in the plane of the films. The values for the TSP were extracted by fitting the data curves with the following fitting parameters[6,7,12] indicated in the figure: superconducting gap Δ, depairing parameter ζ, and spin-orbit parameter b.

Consistent with these high TMR values, superconducting tunnelling spectroscopy experiments confirm that (100)-oriented MgO tunnel structures have a spin polarization of ~85% at low temperature. Improved crystal perfection and orientation are very likely to lead to even higher TMR values. The high TMR of these structures, together with the ability to build complex magnetically engineered structures from these materials, suggests that these materials will have a major impact on technologically relevant spintronic devices operable at room temperature and above in the near future. For example, higher signal strengths from higher TMR values might make easier the implementation of advanced MRAM architectures such as the ultra-dense cross-point random access memory[29].

METHODS

SAMPLE PREPARATION

The STS samples were fabricated using shadow masks with a superconducting $Al_{96}Si_4$ layer formed on top of the MgO tunnel barrier (C. Kaiser and S. S. P. Parkin, unpublished work). To prevent electrical shorting of the MgO tunnel barrier by the AlSi layer, the edges of the lower ferromagnetic electrode, which consisted of layers of Ta (75 to 100 Å) and IrMn (250Å) and either bilayers of 8 Å $Co_{84}Fe_{16}$/ 18 Å Fe or single layers of 35 Å $Co_{70}Fe_{30}$, were electrically isolated from the AlSi layer by ~200-Å-thick layers of either Al_2O_3 or MgO.

EXPERIMENTAL PROCEDURES

Transmission electron microscopy was carried out on a 200 kV JEOL 2010F field-emission microscope with a lattice resolution down to ~1 Å. The specimens were prepared using conventional cross-sectioning dimpling and ion milling. The MTJs and STS junctions were annealed in a high vacuum (~10^{-8} torr) anneal oven in a field of 0.1 T. Each of the MTJ and STS devices was annealed at a series of increasing anneal temperatures for 30 min at each temperature indicated. Successive anneal temperatures were increased by typically 20 °C. Note that TMR and TSP are often related by Julliere's formula[3], TMR = $2P_1^1P_T^2/(1 - P_1^1P_T^2)$, where P_1^1 and P_T^2 are the TSP values of the current tunnelling from the two sides of the tunnelling barrier. The thicknesses of the layers in the MTJ samples are inferred from mechanical profilometry measurements of the thicknesses of ~500-Å-thick calibration films deposited in the same deposition run as the MTJ devices. The CIPT measurements were carried out on a CAPRES microprobe tool specifically developed for these measurements. The tool is limited to measurements at ambient temperature. The TMR of the shadow-masked MTJs was measured using a standard four-probe geometry. The shadow masked junctions had areas ranging from 20 × 20 to 80 × 80 μm^2.

Received 5 July 2004; accepted 4 October 2004; published 31 October 2004.

References

1. Parkin, S. S. P. *et al.* Magnetically engineered spintronic sensors and memory. *Proc. IEEE* **91,** 661–680 (2003).
2. Parker, J. S., Watts, S. M., Ivanov, P. G. & Xiong, P. Spin polarization of CrO_2 at and across an artificial barrier. *Phys. Rev. Lett.* **88,** 196601 (2002).
3. Julliere, M. Tunneling between ferromagnetic films. *Phys. Lett. A* **54,** 225–226 (1975).
4. Moodera, J. S., Kinder, L. R., Wong, T. M. & Meservey, R. Large magnetoresistance at room temperature in ferromagnetic thin film tunnel junctions. *Phys. Rev. Lett.* **74,** 3273–3276 (1995).
5. Miyazaki, T. & Tezuka, N. Giant magnetic tunneling effect in Fe/Al_2O_3/Fe junction. *J. Magn. Magn. Mat.* **139,** L231–L234 (1995).
6. Meservey, R. & Tedrow, P. M. Spin-polarized electron tunneling. *Phys. Rep.* **238,** 173–243 (1994).
7. Maekawa, S. & Shinjo, T. (eds) *Spin Dependent Transport in Magnetic Nanostructures* (Taylor & Francis, London, 2002).
8. Sun, J. Z., Abraham, D. W., Roche, K. & Parkin, S. S. P. Temperature and bias dependence of magnetoresistance in doped manganite thin film trilayer junctions. *Appl. Phys. Lett.* **73,** 1008–1010 (1998).

9. Jo, M.-H., Mathur, N. D., Todd, N. K. & Blamire, M. G. Very large magnetoresistance and coherent switching in half-metallic manganite tunnel junctions. *Phys. Rev. B* **61,** R14905–R14908 (2000).
10. O'Donnell, J., Andrus, A. E., Oh, S., Colla, E. V. & Eckstein, J. N. Colossal magnetoresistance magnetic tunnel junctions grown by molecular-beam epitaxy. *Appl. Phys. Lett.* **76,** 1914–1916 (2000).
11. Bowen, M. *et al.* Nearly total spin polarization in $La_{2/3}Sr_{1/3}MnO_3$ from tunneling experiments. *Appl. Phys. Lett.* **82,** 233–235 (2003).
12. Worledge, D. C. & Geballe, T. H. Maki analysis of spin-polarized tunneling in an oxide ferromagnet. *Phys. Rev. B* **62,** 447– 451 (2000).
13. Parkin, S. S. P., More, N. & Roche, K. P. Oscillations in exchange coupling and magnetoresistance in metallic superlattice structures: Co/Ru, Co/Cr and Fe/Cr. *Phys. Rev. Lett.* **64,** 2304–2307 (1990).
14. Wang, D., Nordman, C., Daughton, J. M., Qian, Z. & Fink, J. 70% TMR at room temperature for SDT sandwich junctions with CoFeB as free and reference layers. *IEEE Trans. Magn.* **40,** 2269–2271 (2004).
15. Mavropoulos, P., Papanikolaou, N. & Dederichs, P. H. Complex band structure and tunneling through ferromagnet/insulator/ferromagnet junctions. *Phys. Rev. Lett.* **85,** 1088–1091 (2000).
16. Butler, W. H., Zhang, X.-G., Schulthess, T. C. & MacLaren, J. M. Spin-dependent tunneling conductance of Fe|MgO|Fe sandwiches. *Phys. Rev. B* **63,** 054416 (2001).
17. Mathon, J. & Umerski, A. Theory of tunneling magnetoresistance of an epitaxial Fe/MgO/Fe(001) junction. *Phys. Rev. B* **63,** 220403 (2001).
18. Bowen, M. *et al.* Large magnetoresistance in Fe/MgO/FeCo(001) epitaxial tunnel junctions on GaAs(001). *Appl. Phys. Lett.* **79,** 1655–1657 (2001).
19. Faure-Vincent, J. *et al.* High tunnel magnetoresistance in epitaxial Fe/MgO/Fe tunnel junctions. *Appl. Phys. Lett.* **82,** 4507–4509 (2003).
20. Yuasa, S., Fukushima, A., Nagahama, T., Ando, K. & Suzuki, Y. High tunnel magnetoresistance at room temperature in fully epitaxial Fe/MgO/Fe tunnel junctions due to coherent spin-polarized tunneling. *Jpn J. Appl. Phys.* 43, L588–L590 (2004).
21. Worledge, D. C. & Trouilloud, P. L. Magnetoresistance measurement of unpatterned magnetic tunnel junction wafers by current-in-plane tunneling. *Appl. Phys. Lett.* **83,** 84–86 (2003).
22. Simmons, J. G. Generalized formula for the electric tunnel effect between similar electrodes separated by a thin insulating film. *J. Appl. Phys.* **34,** 1793–1803 (1963).
23. Mitani, S., Moriyama, T. & Takanashi, K. Fe/MgO/FeCo(100) epitaxial magnetic tunnel junctions prepared by using *in situ* plasma oxidation. *J. Appl. Phys.* **93,** 8041–8043 (2003).
24. Kiyomura, T., Maruo, Y. & Gomi, M. Electrical properties of MgO insulating layers in spin-dependent tunneling junctions using Fe3O4. *J. Appl. Phys.* **88,** 4768–4771 (2000).
25. Bredow, T. & Gerson, A. R. Effect of exchange and correlation on bulk properties of MgO, NiO, and CoO. *Phys. Rev. B* **61,** 5194–5201 (2000).
26. Pedersen, R. J. & Vernon, F. L. Effect of film resistance on low-impedance tunneling measurements. *Appl. Phys. Lett.* **10,** 29–31 (1967).
27. Veerdonk, R. J. M. v. d., Nowak, J., Meservey, R., Moodera, J. S. & Jonge, W. J. M. d. Current distribution effects in magnetoresistive tunnel junctions. *Appl. Phys. Lett.* **71,** 2839–2841 (1997).
28. De Teresa, J. M. *et al.* Role of metal-oxide interface in determining the spin polarization of magnetic tunnel junctions. *Science* **286,** 507–509 (1999).
29. Reohr, W. *et al.* Memories of tomorrow. *IEEE Circuits Device* **18,** 17–27 (2002).
30. Meyerheim, H. L. *et al.* Geometrical and compositional structure at metal-oxide interfaces: MgO on Fe(001). *Phys. Rev. Lett.* **87,** 076102 (2001).

Acknowledgements

We thank Daniel Worledge for the CIPT measurements. Christian Kaiser is also at RWTH Aachen, Physikalisches Institut (IIA), 52056 Aachen, Germany. This work is partially supported by the DARPA spintronics and SPINS programs.
Correspondence and requests for materials should be addressed to S.S.P.P

Competing financial interests

The authors declare that they have no competing financial interests.